NOEMOL: integrated molecular graphics and the simulation of Nuclear Overhauser effects in NMR spectroscopy

Mark Forster, Chris Jones and Barbara Mulloy

National Institute for Biological Standards and Control, Hertfordshire, UK

Nuclear Overhauser effects (NOEs) are a widely used method of determining the spatial proximity of spins in Nuclear Magnetic Resonance (NMR) spectroscopy. This paper describes a C program developed for the Sun-3 workstation family that allows the computation of multispin NOE effects for a given molecular structure and given NMR parameters (i.e., resonance frequency and correlation time for molecular reorientation). The integration of these facilities with simple molecular graphics display routines allows modifications to the molecular conformation (such as bond rotations) to be performed, and the effect of these modifications on the NOE effects can then be rapidly calculated and easily visualized. Using the Sun windowing system, the NOE effects can be calculated for two (or more) candidate structures and compared to experimental NMR results. The overall molecular reorientation can be modeled by either isotropic or symmetric top diffusion models, and the internal motions of methyl groups are modeled using an algorithm reported by Tropp.

Keywords: molecular graphics, nuclear magnetic resonance (nmr), Nuclear Overhauser effect (NOE).

INTRODUCTION

High-resolution Nuclear Magnetic Resonance (NMR) is an established method for obtaining dynamic and structural information about molecules in the solution state.[1] Nuclear Overhauser effects (NOEs) in NMR spectroscopy can be defined as the fractional change in the peak area of a resonance, when the equilibrium magnetization of one or more other resonances is perturbed by an irradiating radio-frequency (RF) field. For any given spin i, two types of interaction constant must be distinguished. The cross relaxation rate constant σ_{ij} describes the rate at which any perturbation in the equilibrium magnetization passes between the two spins i and j. The auto relaxation rate ρ_j determines the rate at which spin i loses magnetization to the lattice or bath, and hence returns to equilibrium. NOE experiments can frequently provide detailed information on the spatial proximity of spins due to the r^{-6} dependence of the cross relaxation rate upon distance.[2,3]

For a system of two spins, the time course for an NOE can be calculated as an analytical function of the ρ and σ parameters. For systems of more than two spins, multiple relaxation pathways become operative and a simple analytical function cannot be found. The problem is compounded when macromolecules are being studied and the time scale for molecular reorientation (characterized by a correlation time τ_c) is slow compared to the resonance frequency ω_0. Cross relaxation rates then become large and negative and multiple cross relaxation pathways are favored, which leads to a loss in specificity of the NOE transfer, a phenomenon known as spin diffusion.

In order to predict the effects of molecular structure and correlation time on NOEs in the presence of spin diffusion, a full multispin NOE simulation is essential. Several authors have previously used NOE simulations as part of their investigations of molecular structure by NMR.[4–6] The program NOEMOL combines multispin NOE simulation routines with simple molecular graphics display, rotation and manipulation routines, thus allowing interactive structural modification and visualization of these effects on the predicted NOE time course. NOEMOL is written in C and runs on Sun-3 workstations with color graphics facilities. The procedure for calculating multispin NOE time courses is a

Address reprint requests to Dr. Forster at the National Institute for Biological Standards and Control, Blanche Lane, South Mimms, Potters Bar, Hertfordshire, EN6 3QG, UK.
Received 25 April 1989; accepted 21 June 1989

three-stage process. First, the cross and auto relaxation rate constants (σ_{ij} and ρ_i; $i,j = 1,2..n$) are calculated from a given set of coordinates and a measured or assumed correlation time. Second, the form of the applied perturbation must be determined, which involves selecting which spin(s) are initially inverted or saturated and which spins are saturated during the NOE time course. Lastly, the set of coupled ordinary differential equations governing the time dependence of the z magnetization must be solved.

CALCULATING RELAXATION PARAMETERS

The simplest motional model that can be used for calculating relaxation parameters is the isotropic reorientation rigid body model. With this model all internuclear vectors are governed by the same correlation time. For inequivalent spins i and k separated by a distance r_{ik}, the cross relaxation rate σ_{ik} is[2]

$$\sigma_{ik} = \left(\frac{\mu_0}{4\pi}\right)^2 \frac{\gamma_i^2\gamma_k^2\hbar^2}{10\ r_{ik}^6}\ [6J(\omega_i + \omega_k) - J(\omega_i - \omega_k)] \tag{1}$$

where γ_i, γ_k are the nuclear gyromagnetic ratios, μ_0 is the permeability of free space ($4\pi \times 10^{-7}$ H/m), $\hbar$ is Planck's constant divided by 2π and the spectral density function $J(\omega)$ is

$$J(\omega) = \frac{\tau_c}{1 + \omega^2\tau_c^2} \tag{2}$$

Equivalent spins effectively have no cross relaxation between them. For two protons separated by a distance of 1 Å, the collection of constants preceding the spectral density terms in equation 1 reduces to a value of $5.6965 \times 10^{10}\ s^{-2}$.

The auto relaxation rate ρ_i is a sum of pairwise interaction terms.

$$\rho_i = \sum_{k \neq i} \rho_{ik} \tag{3}$$

where ρ_{ik} is given by

$$\rho_{ik} = \left(\frac{\mu_0}{4\pi}\right)^2 \frac{\gamma_i^2\gamma_k^2\hbar^2}{10\ r_{ik}^6}\ [3J(\omega_i) + 12J(\omega_i + \omega_k)] \tag{4}$$

for equivalent spins,[2] and by

$$\rho_{ik} = \left(\frac{\mu_0}{4\pi}\right)^2 \frac{\gamma_i^2\gamma_k^2\hbar^2}{10\ r_{ik}^6}\ [6J(\omega_i + \omega_k) + J(\omega_i - \omega_k) + 3J(\omega_i)] \tag{5}$$

for inequivalent spins.[2] In NOEMOL spins are considered equivalent if they satisfy one of two criteria. First, both spins must be methyl protons in the same methyl group, and second, they must possess the same atom name, residue name and residue number. This latter rule allows, for example, for the presence of both equivalent and inequivalent methylene protons depending upon the atom names. Relaxation rates σ_{ij} and ρ_i are arranged to form the off diagonal and diagonal elements of the relaxation matrix.

The rigid body model is a simple but rather unrealistic approximation; all molecules possess internal motions that also affect the magnitude of relaxation interactions. The problem of how to incorporate these motions into our calculations is a difficult one, but simple models exist for limiting cases that depend upon the timescale of the motion(s). Typical molecular reorientational correlation times range from picoseconds to nanoseconds, while relaxation rates σ,ρ usually range from a fraction of, to several, seconds. Carver and coworkers[7] have discussed the existence of "virtual conformations" in oligosaccharides, arising from internal motions characterized by correlation times τ_{int} that satisfy

$$\tau_c << \tau_{int} << \sigma_1\rho \tag{6}$$

Motions in the microsecond to millisecond time range would be expected to be well described by this model. This approach is equivalent to calculating r_{ik}^{-6} for the appropriate spin pair in each allowed conformation and taking a Boltzmann weighted average of these values.

Motions that are fast compared to overall reorientation, such as methyl group rotations, pose another problem. Clearly, such motions average the distance from a fixed proton to a methyl proton; however, taking a simple average of r^{-6} is not appropriate and has no theoretical basis. Tropp[8] has reported a general model for calculating the effect of fast internal motions, the essence of which is discussed here. If the spin–spin vector is assumed to "jump" rapidly between n equally populated conformations, each conformation being characterized by a distinct spin–spin distance r_{ik} and angles θ_{ik} and ϕ_{ik} defining the orientation of the spin–spin vector. In such a case the distance terms r_{ik}^{-6} given above are replaced by

$$\langle 1/r^6\rangle_{eff} = \sum_{m=-2}^{+2} f(m)$$

$$f(m) = \left|\sum_{j=1}^{n} \frac{Y_{2m}(\theta_{ik}, \phi_{ik})}{n\ r_{ik}^3}\right|^2 \tag{7}$$

where Y_{2m} are the spherical harmonic functions that can more conveniently be expressed in Cartesian coordinates.[9] NOEMOL models CH_3 group internal rotations using a 3-site jump model. Therefore, fixed proton–methyl proton interactions are subjected to 3-site averaging while the interaction of two methyl protons in distinct methyl groups requires 9-site averaging. It should be noted that for a spin–spin vector that reorients but maintains a fixed interspin distance, the averaging implicit in equation (7) leads to an "effective distance" average $\langle 1/r^6\rangle_{eff}$ that can be considerably less than r_{ik}^{-6}. As an example, the interaction between two methyl protons in the same methyl group jumps between three conformations. In the case of isotropic overall reorientation, the effective distance average $\langle 1/r^6\rangle_{eff}$ can be shown to be $\frac{1}{4}r_{HH}^6$ and to be independent of methyl group orientation.

For systems in which overall isotropic reorientation is unlikely, the next simplest model that can be applied is that

of a symmetric top rotor. For this model two distinct correlation times $\tau_{\parallel}$ and $\tau_{\perp}$ are required to describe motion about the symmetric top axis and about an axis perpendicular to it, respectively. For proton–proton vectors rigidly held in the symmetric top framework, equation (2) is replaced by the equations described by Woessner[10]

$$J(\omega) = \tfrac{1}{4}(3\cos^2\theta - 1)^2\,\tau_{20}/(1 + \omega^2\tau_{20}^2) + 3\cos^2\theta\sin^2\theta\,\tau_{21}/(1 + \omega^2\tau_{21}^2) + \tfrac{3}{4}\sin^4\theta\,\tau_{22}/(1 + \omega^2\tau_{22}^2) \quad (8)$$

where θ is the angle between the spin–spin vector and the symmetric top axis. The correlation times τ_{20}, τ_{21}, τ_{22} are defined as

$$1/\tau_{2m} = 6D_{\perp} + m^2(D_{\parallel} - D_{\perp})$$
$$D_{\perp} = \tfrac{1}{6}\tau_{\perp} \quad (9)$$
$$D_{\parallel} = \tfrac{1}{6}\tau_{\parallel}$$

The D values are diffusion constants.

If the spin–spin vector is not fixed in the symmetric top framework but jumps rapidly between conformations (i.e., if one of the spins is a methyl proton), then for a symmetric top the distance and spectral density terms cannot be separated. The previously used product of $r^{-6}J(\omega)$ is replaced by the new spectral density function

$$J(\omega) = \sum_{m=-2}^{+2} \frac{\tau_{2m} f(m)}{1 + \omega^2\tau_{2m}^2} \quad (10)$$

This equation reduces to equations (8), (7) and (2) in the appropriate limits. Note that while $f(m)$ is still defined as in equation (7), the angles θ_{ik} and ϕ_{ik} are now measured relative to the symmetric top axis. In the isotropic rotor case any axis system (including the laboratory axes) could have been used. NOEMOL allows the simulation of ^1H–^1H NOEs for spherical and symmetric top reorientation models and models CH_3 internal rotations using the Tropp formalism.

SOLUTION OF TIME COURSE EQUATIONS

The time dependence of the z magnetization for a given spin i in a multispin system is described by equations due to Solomon.[2,11]

$$\frac{d}{dt}\eta_i = -\rho_i\eta_i - \sum_{k\neq i}\sigma_{ik}\eta_k \quad (11)$$

where $i = 1, 2 \ldots n$ and η_i is the NOE for spin i.

The description of the NOE experiment to be simulated involves specifying which spins are initially inverted, which are initially saturated and which are saturated throughout the timecourse. The solution to equation 11 gives the time dependence of all the NOEs and is obtained by numerically integrating this set of coupled ordinary differential equations. In NOEMOL this integration is achieved by using the 4th order Runge–Kutta method with adaptive step size control, rather than the conceptually simpler but less efficient Euler method.[12,13] The initial integration step size is set to the lesser of $\frac{1}{10}\rho_{max}$ (ρ_{max} is the largest of the calculated ρ values) or $t'/10$ (t' being the simulation time interval at which NOE data is stored during the timecourse). During the integration the step size is adjusted to maintain a maximum fractional error of 1 part in 10^4. This is far higher than error with which experimental NOEs can be determined.

PROGRAM IMPLEMENTATION

NOEMOL was written in C and is intended to be used in a graphics tool window under the Suntools window environment of the Sun-3 series workstation. The graphics display routines were implemented using the SunCGI graphics library package.[14] This simple two-dimensional display library offers faster drawing and a greater range of drawing primitives and attributes than the SunCORE library, but it does not support segmentation and transformations. The simplicity of the CGI primitives should be an aid to future portability of the code. Rather than introduce additional machine specific features, NOEMOL uses a simple command-line interpreter (CLI) to accept commands from the text subwindow of the graphics tool window. This allows standard C language input/output to be used for command processing.

The program supports several display options including vector displays in a single color or in a color-coded half-bond representation. Ball-and-stick and simple space-filling displays have also been incorporated. A utility program is used to load PDB format files, generate atom–atom connectivities using a simple distance criterion and generate a disk file containing atom and connectivity data for use by NOEMOL. This saves the computational burden of generating connectivity data each time a structure is loaded. In the present version only hydrogen atoms are accepted as NMR active spins. The connectivity information is then used to automatically distinguish between methyl and nonmethyl protons, as these are handled differently in calculating the relaxation matrix. Atom information, distances, bond angles and torsion angles can be obtained by picking atoms with the cursor. Overall x, y, z rotations, scaling and bond rotations are supported. Naturally, altering a structure by bond rotations invalidates any previously calculated relaxation matrix. The ρ value for a single spin or the σ value for a pair of spins can be calculated without recourse to a full relaxation matrix calculation. If the full relaxation matrix has been calculated, initial perturbation (inversion, saturation) conditions can be set along with the identity of the spin(s) to be saturated throughout the timecourse. The calculation of a relaxation matrix for a set of 46 spins takes approximately 120 seconds on our Sun-3/160 workstation, while integration of a 20-point NOE timecourse for the same set of spins typically takes about 75 seconds. Thus, the program is sufficiently fast for interactively simulating the NOE timecourse for macromolecules. Following integration, the NOE timecourse for individual spins can then be listed in the text subwindow or displayed in the graphics subwindow. A list of the commands accepted by the simple CLI is given in Table 1. NOEMOL interfaces to external data processing and graphics packages by simply using ASCII data files as an output medium. We are currently using the SAS/GRAPH™ package to generate NOE timecourse plots and contour plots of selected NOE parameters as a function of two torsion angles.

Table 1. Commands accepted by the NOEMOL command-line interpreter

ve1:	Vector display 1—one color only
ve2:	Vector display 2—color coded half-bond representation
bst:	Ball-and-stick display
sm1:	Space filling model 1—one color only
sm2:	Space filling model 2—circles representing atoms are color-coded
tau:	Enter new effective reorientational correlation time(s)
axis:	Pick pair of atoms defining symmetric top axis
angl:	Give angle between atom-atom pair and top axis
rho:	Calculate ρ value for spin picked by cursor
sig:	Show σ value for pair of spins
mat:	Calculate relaxation matrix (i.e., complete set of ρ and σ values)
lrm:	List row/column of relaxation matrix
noe:	Set up perturbation and saturation conditions. Integrate Solomon equations and obtain NOE timecourse for all spins
lno:	List NOE timecourse in text subwindow
dno:	Display NOE timecourse in graphics subwindow
wno:	Write ASCII file of NOE data to disk
rx, ry, rz:	Enter rotation angle and perform x,y, or z rotation, respectively
sc:	Set new display scaling factor
br:	Pick two atoms, enter angle and perform bond rotation
pa:	Pick atom, show atom number, residue name and number and spin number (zero if not a hydrogen)
di:	Distance between two picked atoms
ba:	Bond angle between three picked atoms
tor:	Torsion angle calculation
bc:	Check for, and display, bad atom–atom contacts
vdw:	Calculate vdw energy using simplified MM2 force field
conl:	Generate contour plot data for display of inter-spin distance or σ against torsion angles
quit:	Quit NOEMOL

COMPARISON OF CALCULATED AND EXPERIMENTAL NMR DATA

One use of a program such as NOEMOL is to attempt to evaluate the quality of proposed structures by comparison of experimental and calculated NOE data. One factor that must be emphasized is that calculated σ and NOE values are extremely sensitive functions of the structure. Because of this, quite small variations or errors in distances should be readily detectable. Examples of NOE simulations involving molecules currently under study in this laboratory follow.

Phenolic trisaccharide

Phenolic glycolipids are known to constitute species-specific surface antigens for a number of mycobacteria. In the bacterium *M. leprae*, responsible for the disease leprosy, the abundant phenolic glycolipid contains a trisaccharide moiety

$$3,6(OMe)_2\beta DGlc(1\text{–}4)\text{–}$$
$$2,3(OMe)_2\alpha LRha(1\text{–}2)\text{–}3OMe\alpha LRha(1\text{–})$$

which is linked via a phenyl group to a lipid core. Here we shall discuss a few details of the solution structure of a synthetic phenolic trisaccharide with the above structure. The $2,3(OMe)_2\alpha$Rha and $3OMe\alpha$Rha saccharides will be referred to as *B* and *C*, respectively. The structure about this glycosidic linkage has been investigated by ^1H–$\{^1H\}$ NOE methods as well as by long range ^{13}C–^1H coupling constant experiments.[15,16] The measured ^{13}C–^1H coupling of 4.3 Hz between H1*B* and C2*C* implies possible torsion angles of $\pm 139°$ and $\pm 28°$ for H1*B*-C1*B*-O2*C*-C2*C*. A two-dimensional NOESY experiment (mixing time 0.9 seconds) showed cross peaks from H1*B* to H2*B* and H2*C* but not from H1*B* to H1*C* or H3*C*. A one-dimensional NOE timecourse, obtained by irradiating H1*B* for varying lengths of time, allowed the cross relaxation rates σ(H1*B*-H2*B*) and σ(H1*B*-H2*C*) to be measured as $-0.140 \pm 0.014\,s^{-1}$ and $-0.203 \pm 0.007\,s^{-1}$, respectively. An isotropic reorientational correlation time of 0.86 ns was derived from the H1*B*-H2*B* distance of 2.60 Å. NOEMOL was used to generate contour data representing σ(H1*B*-H2*C*) as a function of the glycosidic torsion angles (Figure 1). Although a contour plot of the H1*B*-H2*C* distance could have been used in this case, we prefer to view σ directly since this is the experimentally determined variable. In addition, the presence of internal motions or anisotropic overall reorientation will perturb the direct r^{-6} relationship between distance and σ, thus making distance plots less useful. The torsion angles of $\pm 139°$ are seen to be inconsistent with the measured σ value. The torsion angles $\pm 28°$ intersect the measured σ value at four points in the torsion angle space (Figure 1). Points 1 and 2 can be rejected since they correspond to short (<2 Å) H1*B*-H1*C* distances and would lead to large observed NOEs. Point 3 can be rejected since a bad contact (1.39 Å between H4*C* and H2*B*) leads to a large VDW energy. Thus, point 4 is the only single conformation in the torsion angle space that is consistent with the available data. Calculation of the NOE timecourse observed at H2*C* and H2*B* following saturation of H1*B* shows good agreement between calculated and experimental data (Table 2). Since the cross relaxation rates have been used to constrain the correlation time and the glycosidic torsion angles, the fact that the calculated NOEs are very slightly larger than the experimental ones implies that the calculated auto relaxation rate parameters for spins H2*B* and H2*C* are slightly lower than the true experimental rates. This is as expected since the program calculates only the contribution of intramolecular proton–proton dipolar interactions to the auto relaxation rates. Other minor terms, such as the proton–deuteron dipolar interaction with the deuterated solvent, are neglected since they cannot be easily quantified.

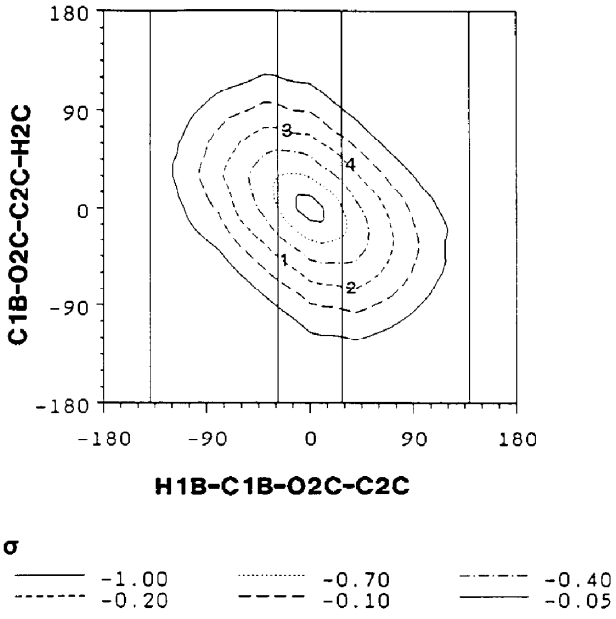

Figure 1. Contour plot of cross relaxation rate σ(H1B–H2C) against glycosidic torsion angles. The vertical bars represent conformations consistent with the long-range carbon–proton coupling constant of 4.3 Hz. The four points marked show conformations mutually consistent with the coupling constant data and with the experimental cross relaxation rate of 0.2 s^{-1}. Evidence allowing points 1,2,3 to be eliminated is discussed in the text

Table 2. Comparison of experimental and calculated NOEs for phenolic trisaccharide compound

	NOE {H1*B*}-H2*C* (%)		NOE {H1*B*}-H2*B* (%)	
t(secs)	Expt.	Calc.	Expt.	Calc.
0.1	−1.8	−1.9	−1.7	−1.3
0.2	−3.4	−3.6	−2.7	−2.5
0.4	−6.1	−6.5	−3.5	−4.4
0.5	−6.9	−7.6	−5.0	−5.2
0.7	−8.8	−9.7	−6.3	−6.5
1.0	−10.0	−11.9	−6.8	−8.0
2.0	−12.3	−15.8	−8.8	−10.5

Heparin derivative

The anticoagulant glycosaminoglycan heparin has a heterogeneous structure but consists largely of a repeating disaccharide unit,

[4)–α–L–IdoA2SO_3^-–(1–4)–
α–D–GlcNSO_3^-6SO_3^-(1–]

This species and its N-desulphated, re-N-acetylated analogue have been studied by ^1H, ^{13}C NMR and molecular mechanics methods. Full details of these studies will be published elsewhere. In order to properly account for spin diffusion effects to neighbor spins, but to limit the total number of spins, we have performed NOE simulations on a hexasaccharide model of the N-desulphated re-N-acetylated heparin derivative consisting of three repeating units. Model *G-I* and *I-G* disaccharides were subjected to a conformation search procedure using a CHEM-X/microvax II modeling system and then energy minimized using the MM2CARB force field. Conformations that were close energetically were distinguished using spin–spin distance vs. torsion angle maps generated by NOEMOL. Disaccharides were then assembled into a model hexasaccharide and this transferred to the Sun-3/160 for NOE simulations. Saturation of a single NMR resonance involves simulating the saturation of three spins. Observation of NOE transfer was limited to spins near the central portion of the hexasaccharide in order to eliminate possible end effects. We have been unable to rationalize the observed NOEs in the N-desulphated re-N-acetylated heparin derivative using an isotropic reorientation model. In particular, the NOEs observed at H2 upon saturating H1 for the *G* (GlcNAc6SO_3^-) and *I* (IdoA2SO_3^-) residues were found to be 20% and 4%, respectively, at 200 ms. These are not compatible with the H1-H2 distances of 2.41 Å and 2.57 Å for *G* and *I*, respectively.

In a symmetric top rotor the cross relaxation rates are dependent upon both the spin–spin distance and the angle between the spin–spin vector and the top axis. Defining the symmetric top axis as the vector joining the end anomeric carbons in our hexasaccharide model, we have found these angles to be approximately 14° and 87° for the *G* and *I* H1–H2 vectors, respectively. Using reorientation parameters of 5 ns for $\tau_\perp$ and 25 for the ratio $\tau_\perp/\tau_\parallel$ leads to reasonably good agreement between the calculated and experimental NOEs for this system (Table 3). In our hexasaccharide model we have used the predominant $^1C_4$ chair structure for the IdoA2SO_3^- moiety; using the minor $^2S_0$ skew boat conformation generates a slightly smaller IdoA H1–H2 NOE but makes little difference to any of the other experimentally observed NOEs. Calculated NOE timecourses

Table 3. Calculated and experimental NOE data for heparin derivative

Spin	Experimental NOE (%)	Calculated NOE (%)
Saturate H1*G* for 200 ms.		
H2G	−20	−22
H3I	−17	−24
H4I	Small	−1
Saturate H1*I* for 200 ms.		
H2I	−4	−4
H4G	−4	−3
H6SG, H6RG	Combined −10	−8 −3

Note that the H6S and H6R protons overlap in the experimental ^1H NMR spectrum; hence, only the combined NOE of −10% can be measured. The residue abbreviations *I* and *G* represent the IdoA2SO_3^- and GlcNAc6SO_3^- groups, respectively

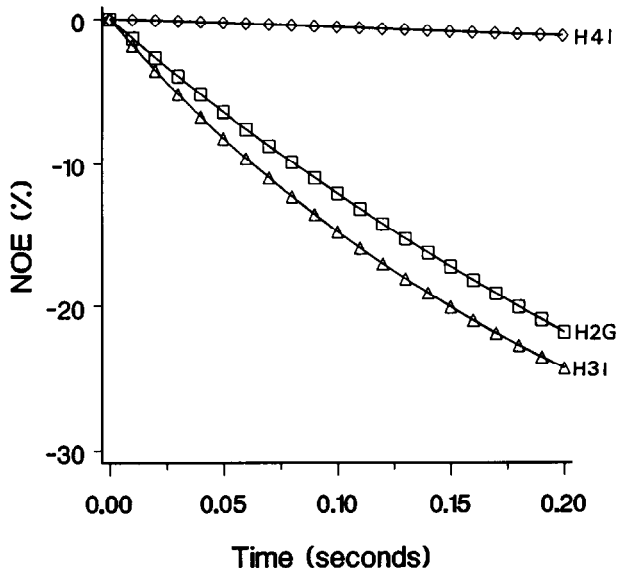

*Figure 2. Calculated NOE timecourse curves for H4*I, *H3*I *(*I *is resi-due IdoA2SO$_3^-$) and H2*G *(*G *is residue Glc-NAc6SO$_3^-$) protons of the N-desulphated re-N-acetylated heparin derivative following saturation of H1*G. *Symmetric top reorientation model used with parameters* $\tau_\perp = 5$ *ns,* $\tau_\perp/\tau_\parallel = 25$

for H4*I*, H3*I* and H2*G* upon saturating H1*G* are shown in Figure 2.

FUTURE DEVELOPMENTS

Several areas in which NOEMOL could be extended or improved are under consideration. A greater degree of display hardware independence could be provided by use of an industry-standard graphics library such as PHIGS. Versions of NOEMOL for other machines could be developed quite simply. The inclusion of other NMR related calculations such as ^{13}C T_1, T_2 and ^{13}C-{^1H} NOE values would be relatively straightforward and would allow both ^1H and ^{13}C NMR data to be used simultaneously to test correlation times and molecular structures.

ACKNOWLEDGEMENTS

The authors wish to thank Roy Gigg and Sheila Payne of the National Institute for Medical Research, Mill Hill, London, for the synthesis of the synthetic phenolic trisaccharide. Nuclear Magnetic Resonance experiments were carried out on the Bruker AM500 spectrometer of the M.R.C. biomedical NMR center at the National Institute for Medical Research. We thank Dr. E. A. Johnson of N.I.B.S.C. for the preparation of the heparin derivative. We also acknowledge the use of CHEM-X, developed and distributed by Chemical Design Ltd., Oxford, UK.

REFERENCES

1 Wuthrich, K. *NMR of Proteins and Nucleic Acids.* J. Wiley and Sons, New York, 1986
2 Macura, S. and Ernst, R.R. *Mol. Phys.* 1980, **41,** 95
3 Noggle, J.H. and Schirmer, R.E. *The Nuclear Overhauser Effect.* Academic Press, New York, 1971
4 Lane, A.N. *J. Magn. Reson.* 1988, **78,** 475
5 Keepers, J.W. and James, T.L. *J. Magn. Reson.* 1984, **57,** 404
6 Dobson, C.M., Olejniczak, E.T., Poulsen, F.M. and Ratcliffe, R.G. *J. Magn. Reson.* 1982, **48,** 97
7 Cumming, D.A. and Carver, J.P. *Biochem.* 1987, **26,** 6664
8 Tropp, J. *J. Chem. Phys.* 1980, **72,** 6035
9 Weissbluth, M. *Atoms and Molecules* (student edition). Academic Press, New York, 1978
10 Woessner, D.E. *J. Chem. Phys.* 1962, **37,** 647
11 Solomon, I. *Phys. Rev.* 1955, **99,** 559
12 Press, W.H., Flannery, B.P., Teukolsky, S.A. and Vetterling, W.T. *Numerical Recipes in C, the Art of Scientific Computing.* Cambridge University Press, 1988
13 Gear, C. *Numerical Initial Value Problems in Ordinary Differential Equations.* Prentice Hall, Englewood Cliffs, NJ, 1971
14 Sun CGI reference manual, Revision B (1986), Sun Microsystems, Inc., 2250 Garcia Ave., Mountain View, CA 94043, USA
15 Mulloy, B.M., Frenkiel, T.A. and Davies, D.B. *Carbohydr. Res.* 1988, **184,** 39
16 Tvaroska, I., Hricovini, M. and Petrakova, E. *Carbohydr. Res.*, 1989, **189,** 359